Two-Quantum Transitions in the Microwave Magnetic Resonance Spectrum of Atomic Chlorine*

GEORGE J. WOLGA†
Research Laboratory of Electronics, Massachusetts Institute of Technology, Cambridge, Massachusetts
(Received January 22, 1962)

Two-quantum microwave magnetic resonance transitions corresponding to $\Delta M_J=\pm 2$ have been observed for both stable isotopes of atomic chlorine, Cl^{35} and Cl^{37}. The experimentally observed and theoretically predicted positions of the two-quantum transitions agree within 13 parts per million, which was the precision of the experiment. The power dependence of the two-quantum transitions has been measured and checked with a "variation of constants" treatment of the microwave-induced probability amplitudes, and agreement has been found. Variations in intensity between corresponding $\Delta M_J=\pm 1$ and $\Delta M_J=\pm 2$ resonances were observed and analyzed on the basis of time-dependent perturbation theory and the Schwinger-Karplus expression for the line shape of a collision-broadened resonance with saturation. Satisfactory agreement with theory is found for these intensity variations. The linewidths for the $\Delta M_J=\pm 2$ lines are approximately half of that for the $\Delta M_J=\pm 1$ lines; this is in agreement with the results of time-dependent perturbation theory.

I. INTRODUCTION

THE ground state $^2P_{\frac{3}{2}}$ of free atomic chlorine has been studied by the method of atomic-beam magnetic resonance spectroscopy,[1,2] and, more recently, by using the method of electron paramagnetic resonance spectroscopy (EMR).[3–6] In the latter method, magnetic dipole transitions are induced in a moderately strong magnetic field (3000–5000 G), which corresponds to $\Delta M_J=\pm 1$, $\Delta M_I=0$ in the high-field quantum-number representation. Hughes and Geiger,[7] elaborating on similar experiments with atomic oxygen, observed additional transitions which they interpreted as the simultaneous absorption of two equi-energetic quanta corresponding to a transition of the type $\Delta M_J=\pm 2$. Hughes and Geiger survey prior observations of two-quantum transitions in nuclear resonance, atomic-beam magnetic resonance, and atomic-beam electric resonance experiments. It is the purpose of this paper to discuss our observation of two-quantum transitions in the ground $^2P_{\frac{3}{2}}$ state of atomic chlorine for both isotopes, Cl^{35} and Cl^{37}.

* This work was supported in part by the U. S. Army Signal Corps, the Air Force Office of Scientific Research, and the Office of Naval Research and was performed under Signal Corps Contract DA-36-039-sc-78108.

† Now at Cornell University, Ithaca, New York.

[1] L. Davis, Jr., B. T. Feld, C. W. Zabel, and J. R. Zacharias, Phys. Rev. **76**, 1076 (1949).

[2] J. H. Holloway, B. B. Aubrey, and J. G. King, Quarterly Progress Report, Research Laboratory of Electronics, Massachusetts Institute of Technology, April 15, 1956 (unpublished), pp. 35–36.

[3] G. J. Wolga and M. W. P. Strandberg, Bull. Am. Phys. Soc. **4**, 153 (1959).

[4] V. Beltran-Lopez and H. G. Robinson, Bull. Am. Phys. Soc. **5**, 273 (1960).

[5] J. S. M. Harvey, R. A. Kamper, and K. R. Lea, Proc. Phys. Soc. (London) **76**, 979 (1960).

[6] V. Beltran-Lopez and H. G. Robinson, Phys. Rev. **123**, 161 (1961).

[7] V. W. Hughes and J. S. Geiger, Phys. Rev. **99**, 1842 (1955).

II. THEORY

A. Atomic Chlorine Energy Levels in a Magnetic Field

The reduced Hamiltonian that was considered is

$$\mathcal{H}/a=(J_Z+\alpha I_Z)x+\mathbf{I}\cdot\mathbf{J}+cQ_{\rm op}, \qquad (1)$$

where

$$Q_{\rm op}=\frac{3(\mathbf{I}\cdot\mathbf{J})^2+(3/2)(\mathbf{I}\cdot\mathbf{J})-I(I+1)J(J+1)}{2I(2I-1)(2J-1)J},$$

$$c=a/b,\quad x=g_J\mu_0H_Z/ha,\quad \text{and}\quad \alpha=(m/M)(g_I/g_J).$$

Here a and b are the hyperfine-structure (hfs) coupling constants. The Hamiltonian that was treated is appropriate to hfs multiplet calculations that are diagonal in J. The omitted terms in the Hamiltonian arising from matrix elements off-diagonal in J and linear in H_Z were compensated for by using for g_J the experimentally determined value 1.333927 in the $^2P_{\frac{3}{2}}$ ground state.[5,6] There is an off-diagonal in J, matrix component of the proper Zeeman term in the Hamiltonian, $\mu_0(g_LL_Z+g_SS_Z)H_Z$, between the $M_J=\pm\frac{1}{2}$ levels in the $^2P_{\frac{3}{2}}$, $^2P_{\frac{1}{2}}$ states. The Zeeman operator can be rewritten as approximately $\mu_0(2J_Z-L_Z)H_Z$, and the nonvanishing off-diagonal matrix elements are

$$-(j,m|L_Z|j-1,m)\mu_0H_Z,$$

where $j=\frac{3}{2}$ and $m=\pm\frac{1}{2}$. These matrix elements are calculated to be equal to $-(2/3)\mu_0H_Z$. Setting up the secular determinant between the $j=\frac{3}{2}$. $M_J=\frac{1}{2}$ and $j=\frac{1}{2}$, $M_J=\frac{1}{2}$ states and solving gives the perturbation of the $j=\frac{3}{2}$, $M_J=\frac{1}{2}$ level as

$$-\frac{2}{9}\frac{\mu_0^2H_Z^2}{\delta}+\frac{4}{81}\frac{\mu_0^4H_Z^4}{\delta^3}+\cdots.$$

The second term may be neglected as exceedingly small and the first in reduced form may be rewritten

as $-ax^2/8\delta$, where δ is the mean or zero field fine-structure splitting. The fine-structure splitting δ for chlorine is 881 $cm^{-1}=2.643\times10^7$ Mc/sec. The correction term is therefore quadratic in H_Z, and has the magnitude $9.706\times10^{-7}x^2$. This term will be seen to be a factor 100 times smaller than the x^2 terms in the Hamiltonian (with only diagonal terms in J included), and is not significant for the precision of this experiment. Therefore it is neglected. The secular equation was formed from the Hamiltonian that is diagonal in J, and solved on the IBM-709 computer at the Computation Center, MIT. The eigenvalues as a function of x were fitted to a power series expansion in x by using the least-squares fitting procedure over a range in x appropriate to the experiment. The least-squares fit was good within a few parts in 10^6, with terms included only to x^2, and the series was terminated at this point. The power-series expansions of the eigenvalues are given in Appendix A. The hfs coupling constants are taken from Holloway, Aubrey, and King,[2] and the nuclear g values from Ting and Williams.[8]

B. Two Quantum Transitions

The theory of these transitions as developed by Hughes and Geiger[7] will prove sufficient to explain the data and is applied here simply to the chlorine problem. The four energy levels under investigation have $M_I=-\frac{3}{2}$ and will be labeled $\frac{3}{2}$, $\frac{1}{2}$, $-\frac{1}{2}$, $-\frac{3}{2}$ to correspond to the M_J value. Assuming that at $t=0$ only the state $|M_J\rangle$ is occupied, we apply the method of "variation of constants" through second order to evaluate the probability amplitude for the state $|M_J+2\rangle$. The quantities entering into the calculation are the time-dependent expansion coefficients $a^S{}_{M_J}(t)$, where S is the order of the calculation. The calculation treats only stimulated absorption, since the transition probability for stimulated emission differs only in the population difference between the upper and lower states. The standard result is

$$\dot{a}_{M_J}{}^{S+1}(t)=\frac{1}{i\hbar}\sum_{M_J'} a_{M_J'}{}^{S}(t)\langle M_J|\mathcal{H}'|M_J'\rangle e^{i\omega_{M_JM_J'}t};$$
$$\omega_{M_JM_J'}=\frac{E_{M_J}-E_{M_J'}}{\hbar} \tag{2}$$

where the transition-inducing perturbation

$$\mathcal{H}'=\boldsymbol{\mu}_{rf}\cdot\mathbf{H}_{rf}=\mathcal{H}'(0)e^{-i\omega t},$$

with the notation of Hughes and Geiger[7] used. Choosing the state $|-\frac{3}{2}\rangle$ to be occupied at $t=0$, we obtain

$$a_{\frac{1}{2}}{}^{(2)}(t)=\frac{-i}{\hbar^2}\frac{\langle\frac{1}{2}|\mathcal{H}'(0)|-\frac{1}{2}\rangle\langle-\frac{1}{2}|\mathcal{H}'(0)|-\frac{3}{2}\rangle}{(\omega-\omega_{-\frac{1}{2}-\frac{3}{2}})}\times\left\{\frac{e^{-i(2\omega-\omega_{\frac{1}{2}-\frac{3}{2}})t}-1}{-i2(\omega-\frac{1}{2}\omega_{\frac{1}{2}-\frac{3}{2}})}-\frac{e^{-i(\omega-\omega_{\frac{1}{2}-\frac{1}{2}})t}-1}{-i(\omega-\omega_{\frac{1}{2}-\frac{1}{2}})}\right\}. \tag{3}$$

[8] Y. Ting and D. Williams, Phys. Rev. **89**, 595 (1953).

Now,

$$\omega_{\frac{1}{2}-\frac{3}{2}}=\omega_{\frac{1}{2}-\frac{1}{2}}+\omega_{-\frac{1}{2}-\frac{3}{2}}. \tag{4}$$

Because of the hyperfine interaction, the levels E_{M_J} are not equally spaced. Therefore $\frac{1}{2}\omega_{\frac{1}{2}-\frac{3}{2}}\neq\omega_{-\frac{1}{2}-\frac{3}{2}}$ and $\frac{1}{2}\omega_{\frac{1}{2}-\frac{3}{2}}\neq\omega_{\frac{1}{2}-\frac{1}{2}}$, so that if the first term in (3) is resonant, the second one is not. Choosing the first term in (3) to be resonant allows the second term to be ignored; this procedure yields the following expression for the time-dependent expansion coefficient arising from a two-quantum transition:

$$a_{\frac{1}{2}}{}^{(2)}(t)=-\frac{i}{\hbar^2}\frac{\langle\frac{1}{2}|\mathcal{H}'(0)|-\frac{1}{2}\rangle\langle-\frac{1}{2}|\mathcal{H}'(0)|-\frac{3}{2}\rangle}{(\omega-\omega_{-\frac{1}{2}-\frac{3}{2}})}\times\left\{\frac{e^{-i(2\omega-\omega_{\frac{1}{2}-\frac{3}{2}})t}-1}{-i2(\omega-\frac{1}{2}\omega_{\frac{1}{2}-\frac{3}{2}})}\right\}. \tag{5}$$

The resonant denominator corresponds to the Bohr energy condition $\hbar\omega=\frac{1}{2}(E_{\frac{1}{2}}-E_{-\frac{3}{2}})$, which is a $\Delta M_J=+2$ transition and is forbidden in first order. The transition is interpreted as arising from the absorption of two equi-energetic quanta. The interesting point is that the absorbed quanta do not conserve energy between initial state and intermediate state ($|-\frac{3}{2}\rangle$, $|-\frac{1}{2}\rangle$), or between intermediate state and final state ($|-\frac{1}{2}\rangle$, $|\frac{1}{2}\rangle$), but the sum of both quanta do conserve energy between initial and final states ($|-\frac{3}{2}\rangle$, $|\frac{1}{2}\rangle$). An analogous development for the other expansion coefficient corresponding to the second two quantum transition gives

$$a_{\frac{3}{2}}{}^{(2)}(t)=\frac{-i}{\hbar^2}\frac{\langle\frac{3}{2}|\mathcal{H}'(0)|\frac{1}{2}\rangle\langle\frac{1}{2}|\mathcal{H}'(0)|-\frac{1}{2}\rangle}{(\omega-\omega_{\frac{1}{2}-\frac{1}{2}})}\times\left\{\frac{e^{-i(2\omega-\omega_{\frac{1}{2}-\frac{1}{2}})t}-1}{-i2(\omega-\frac{1}{2}\omega_{\frac{3}{2}-\frac{1}{2}})}\right\}. \tag{6}$$

For the purposes of comparison, transition probabilities for two-quantum transitions will be taken as $|a_{\frac{1}{2}}{}^{(2)}(t)|^2$ and $|a_{\frac{3}{2}}{}^{(2)}(t)|^2$.

The factor of 2 in the denominator of the bracketed term in (5) and (6), that does not appear in the first order probability amplitudes for $\Delta M_J=\pm1$ transitions, will account for the smaller linewidth that is observed in the two-quantum transitions.

III. EXPERIMENTAL DETAILS

A. Spectrometer

A reflection cavity spectrometer with straight crystal detection was employed. A Varian V-58 klystron that delivered more than 0.1 W when operated in the 300-V mode was frequency-stabilized to the sample cavity. The sample cavity was operated in the TE_{011} cylindrical mode and was very carefully constructed for optimum Q. An unloaded Q greater than 30 000 was achieved by constructing the cavity from a precisely ground cylindrical quartz shell with ground and silvered brass end

plates. The quartz shell was silvered to an approximate thickness of 0.001 in. on the inside, on the flat ends, and for approximately $\frac{1}{8}$ in. on the outside curved surface at both ends. The silvered end plates are soldered with Woods metal to the silvered quartz shell, and the $\frac{1}{8}$-in. silvered bands on the exterior of the shell permitted a bead of solder to be developed which added to the strength and rigidity of the completed cavity. The thin silver coating on the quartz was less than the skin depth of the modulation magnetic field. The cavity end plates had a circular, $\frac{1}{2}$-in. hole on the cylinder axis fitted with a cylindrical, tubular extension that was approximately $\frac{1}{2}$ in. long. The extension served as a waveguide beyond cutoff for the TE_{011} mode and permitted the insertion of a fused quartz tube through which the sample gas flowed. The quartz sample tube lowered the cavity frequency from approximately 9500 Mc/sec to 8937 Mc/sec, which was the operating frequency for this experiment. The The magnetic field was modulated sinusoidally at a rate of 6000 cps with flat, "pancake" modulating coils that were glued to the magnet pole faces. The power reflected from the sample cavity was detected in a 1N23C crystal rectifier, thereby converting the paramagnetic absorption induced amplitude modulation of the microwave carrier to a 6000-cps carrier whose amplitude was proportional to the slope of the paramagnetic line shape as a function of magnetic field. This signal was selectively amplified in a tuned, low-noise, 6000-cps amplifier, phase sensitively detected, and finally followed by an *RC* filter with narrow bandwidth at zero frequency. The resulting dc signal with amplitude proportional to $\partial\chi''/\partial H_Z$ was fed to a strip chart recorder. The low-impedance electromagnet that was used had pole faces of 12-in. diam, and was powered from a current-regulated transistor power supply. The dc magnetic field could be varied linearly with time. The magnetic field was stable to approximately $1:10^5$.

B. Gas Handling System

Molecular chlorine gas was obtained from the Matheson Company. A Matheson pressure regulator on the tank was coupled to a needle valve which, in turn, was connected by an "O-ring Quick-Connect fitting," manufactured by Vactronic Laboratory Equipment, Inc., to a Bourdon leak made from several feet of thin-walled nickel tubing, $\frac{1}{4}$ in. in diam, which was flattened to give the desired flow impedance. The low-pressure end of the Bourdon leak was attached by a Quick-Connect fitting to the glass-quartz gas-conducting system. Since it is inconvenient to dissociate the molecular gas into free atoms within the sample cavity because of the electrical noise produced in a gas discharge, the atoms, once produced, must be conducted to the sample cavity as rapidly as possible. To insure maximum flow velocity with the available pumps, the pumping line on the low-pressure end of the system was kept approximately $\frac{3}{4}$–1 in. in diam, except for the quartz section that passed through the microwave cavity. Connections between the different sections of the system were made with Quick-Connect fittings and Fisher-Porter glass pipe connectors. Vacuum tightness was maintained with rubber O-rings lightly lubricated with Apiezon vacuum grease. It was found that the chlorine did not significantly attack the rubber O-rings, although, in the interest of vacuum tightness, the O-rings were replaced when they became deformed. A glass, liquid-nitrogen cold trap attached with Fisher-Porter glass pipe connectors preceded a Kinney KC-15 two-stage mechanical pump with a pumping speed of 15 cu ft/min. The gas-handling system proved to be convenient, in that, the system could be pumped down below 1μ Hg when it was closed off at the high-pressure end. Other features were: chlorine tank pressure of 1–2 lb gave an operating pressure of several mm Hg; the flow velocity achieved was evidently high enough because there was no problem in observing the free atoms; the system was demountable and portable which made it easier to clean. Also, a demountable system was a necessity in this experiment because the magnet facility was being shared with other experiments. No wall coating such as those that have been described elsewhere were used. Only the quartz tube was cleaned because the free atoms remained in this section from production to observation. Standard glass-cleaning technique was used, with nitric and chromic acids employed.

C. Atom Production

Molecular chlorine was dissociated in an electrodeless, gas discharge operating at 28 Mc/sec. A Hallicrafters model HT-9 transmitter provided approximately 100 W of rf power. The tank circuit of the HT-9 power-amplifier stage was inductively coupled to a shielded twin conductor coaxial cable which, in turn, was matched to an *LC* tank circuit tuned to 28 Mc/sec. Two copper-sheet electrodes connected across this second tank circuit coupled energy into the discharge. Forced air cooling was provided. The entire discharge end of the rf system was enclosed in a nonmagnetic aluminum box that was grounded to the shield of the coaxial cable which, in turn, was at the laboratory ground. Great care must be exercised in this grounding procedure if excessive electrical noise from the gas discharge and from the transmitter is to be suppressed. The aluminum box was supported by nylon bushings that fitted on the quartz sample discharge tube and was located as close as possible to the microwave sample cavity. The design was such that the discharge took place no farther than 3 in. from the center of the microwave cavity. A detailed sketch of the rf discharge section is shown in Fig. 1. It might be worth mentioning that the gas-handling and atom-producing apparatus described above has been used with chlorine, oxygen,

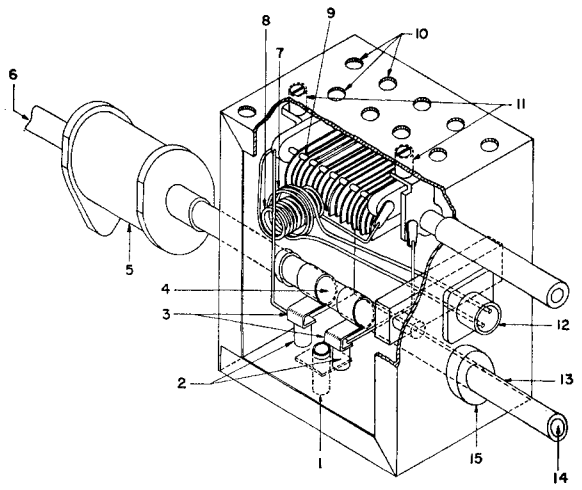

FIG. 1. Radio-frequency discharge apparatus for dissociating chlorine molecules into free atoms. 1, Forced air cooling input; 2, insulating standoffs; 3, copper breakdown electrodes; 4, discharge; 5, microwave cavity; 6, to liquid N_2 trap and pump; 7, primary coil; 8, secondary coil; 9, tuning capacitor; 10, forced air outlet; 11, insulating standoffs; 12, rf input from *HT*-9; 13, quartz tube; 14, chlorine from Bourdon leak; 15, nylon spacer.

hydrogen, and nitrogen with equal success and represents, therefore, what seems to be a universally applicable system for experiments like this one.

D. Magnetic-Field and Klystron-Frequency Measurement

The magnetic field was continuously monitored with a proton resonance probe that was fixed in position in the magnet gap close to the microwave cavity. An Fe_2NO_3-doped water sample was excited by a transistorized marginal oscillator as described by Donnally and Sanders.[9] The marginal oscillator circuit differed from the one referred to above in the substitution of a lower noise audio-frequency transistor amplifier. The proton resonance was modulated at approximately 100 cps with a pair of Helmholtz-like coils attached to the probe with epoxy resin and driven by an audio power amplifier. The coils were made from 1-in. diam rf choke sections. the proton frequency was measured by observing a zero beat between the proton transistor oscillator and a General Radio signal generator whose frequency was directly measured with a frequency counter. The proton resonance magnetic field was not equal to the field at the sample cavity, because of the spatial separation between probe and cavity. However, as will be shown in Sec. V, only differences in resonance fields are pertinent to the experiment, and consequently it was only necessary to maintain a fixed separation between proton probe and sample cavity.

The klystron frequency was measured by coupling a small fraction of the microwave power through coaxial cable to a Hewlett-Packard 540B transfer oscillator, and a zero beat was visually observed on the built-in cathode-ray tube. The transfer-oscillator frequency was measured with the frequency counter by using a Hewlett-Packard 525 Bfrequency converter to extend the frequency range of the counter.

[9] B. Donnally and T. M. Sanders, Jr., Rev. Sci. Instr. **31**, 979 (1960).

E. Microwave Power Measurement

The following procedure was used when observation of the effect of relative changes in microwave power level at the sample was desired. A Hewlett-Packard precision variable attenuator, model X382A, was inserted just before and in series with the detector crystal. A lowest power level was chosen for the experiment and, with the variable attenuator set for zero attenuation, the experiment was run and the detector crystal current was recorded. Then the crystal detector and mount was replaced by a Sperry 821 barretor in a Sperry mount and the power, at the barretor was measured with a Hewlett-Packard 430C microwave power meter. The crystal detector was replaced, a higher power level was chosen, and the experiment was run again. Attenuation was then introduced with the variable attenuator to bring the crystal current back to the starting level and the required amount of attenuation was recorded. Knowledge of this attenuation allowed the original power measurement to be converted to a new value, which was the relative power used in the second run. The process was then repeated for all desired power levels. A check at the lowest power level was made after the variable power runs were completed to see whether or not the crystal had had its conversion properties altered.

IV. EXPERIMENTAL PROCEDURE AND OBSERVATIONS

Two types of experiments were made and each will be described separately.

A. Spectrum Determination

The complete magnetic resonance spectrum at low power for a gas containing both isotopes of chlorine shows 24 resonances; four groups of 3 resonances for each isotope corresponding to the three $\Delta M_J=\pm 1$ transitions for each value of M_I ($\frac{3}{2}$, $\frac{1}{2}$, $-\frac{1}{2}$, $-\frac{3}{2}$). At an operating frequency of nearly 9000 Mc/sec the corresponding groups of resonances overlap for the two isotopes, except for the highest field group corresponding to $M_I=-\frac{3}{2}$. Since the two-quantum transitions were expected to occur at magnetic fields intermediate between the $\Delta M_J=\pm 1$ transitions, as much resolution as possible was desired and consequently all careful work was done on the two $M_I=-\frac{3}{2}$ triplets. A power level was chosen that gave a good signal-to-noise ratio for the two quantum transitions and the magnetic field at resonance was measured for each $\Delta M_J=\pm 1, \pm 2$

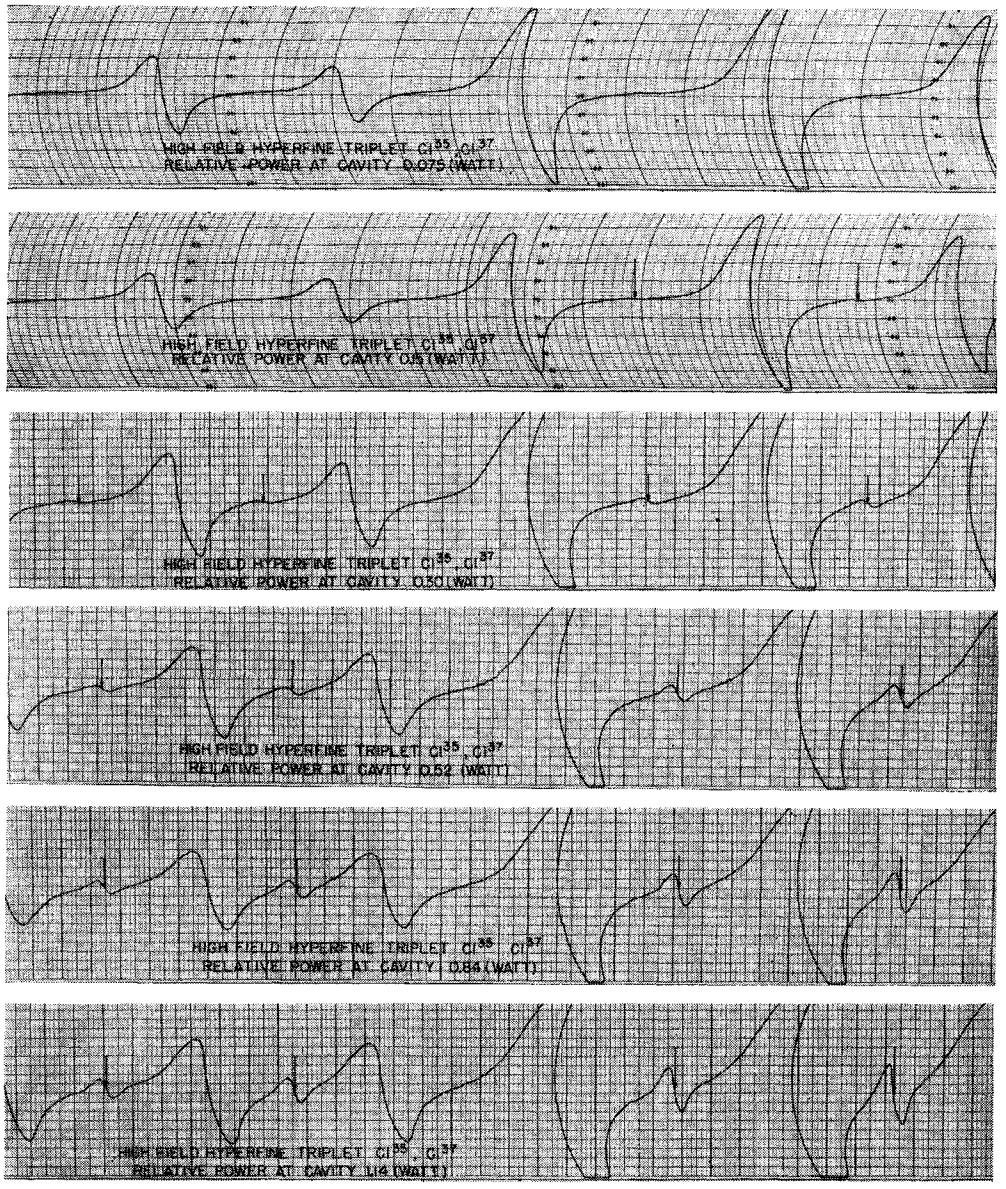

FIG. 2. Microwave transitions for $M_I=-\frac{3}{2}$ and $\Delta M_J=\pm 1$ in atomic chlorine. Resonances for both isotopes are shown; the more intense triplet corresponds to Cl^{35} which is 75% abundant. This figure shows the onset of the two-quantum transitions with increasing microwave power.

transition. This was done by setting the magnetic field at a value midway between the derivative maximum and minimum for a given transition and measuring the proton resonance frequency at this field. The proton resonance was displayed on a cathode-ray oscilloscope with the 100-cps magnetic field modulation amplitude as small as was possible to still yield a clear proton resonance. The frequency of the proton-resonance oscillator was adjusted to put the proton resonance at the center of the sweep and the proton frequency was then measured. This process was repeated approximately ten times for each resonance during a run, and three runs were made. After and before each group of proton frequency measurements, the klystron frequency was measured six or eight times as described in Sec. IIID.

B. Power Dependence of the Spectrum, Intensities, and Linewidths

In these experiments the six $\Delta M_J=\pm 1$ and the four $\Delta M_J=\pm 2$ transitions in the $M_I=-\frac{3}{2}$ groups were studied in detail. Runs were made over a wide range of microwave power. The dc magnetic field was swept linearly in time, and at such a rate that each transition was traversed in a time considerably greater than the detection system time constant. The magnetic field was modulated at 6000 cps with a modulation field amplitude approximately equal to the resonance linewidth. The relative power at the microwave cavity was measured as described in Sec. IIIE. The experimental spectra as a function of power are shown in Fig. 2 (a)

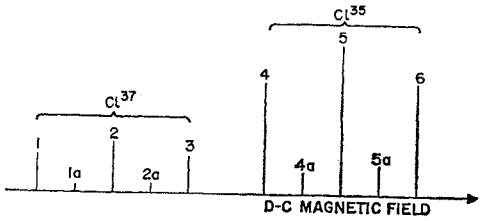

TRANSITION	M_J	M_J'
1,4	1/2	3/2
1a,4a	-1/2	3/2
2,5	-1/2	1/2
2a,5a	-3/2	1/2
3,6	-3/2	-1/2

FIG. 3. Schematic representation of the $M_I=-\frac{3}{2}$ triplets for both Cl^{35} and Cl^{37}, showing relative line positions and intensities.

and (b). The positions of the two-quantum transitions are indicated by vertical arrows. The microwave power notations refer only to relative power at the cavity.

For the purpose of discussion, the spectrum corresponding to $M_I=-\frac{3}{2}$ is represented schematically in Fig. 3.

The linewidth of the two-quantum transitions was noticeably smaller than the $\Delta M_J=\pm 1$ transitions as is to be expected from the theory of two-quantum transitions as presented in Sec. II.

The relative intensity of two-quantum transitions compared with single-quantum transitions as a function of microwave power is summarized in Fig. 4. Intensity is taken as the relative deflection between the maximum and minimum of $\partial\chi''/\partial H_Z$. The intensity of the central $\Delta M_J=\pm 1$ transition is 30% greater than the two neighboring $\Delta M_J=\pm 1$ transitions which have equal intensities. The intensities of each pair of two-quantum transitions are unequal, with the higher field transition

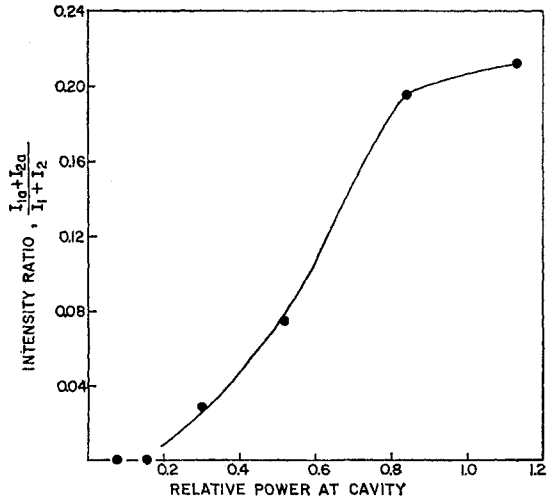

FIG. 4. Relative intensity of two-quantum transitions compared with single-quantum transitions. The intensities used in the ratio are taken from the data of Fig. 2; the line designation refers to Fig. 3.

having greater intensity. This latter effect is not caused by an experimental condition such as a rapid passage alteration of equilibrium between the energy levels, since the same intensity relations were observed when the field sweep began below the group of transitions or above it.

V. TREATMENT OF DATA AND CONCLUSIONS

A. Magnetic Resonance Spectrum

The data available was the klystron or photon frequency and the proton resonance frequency for each of the ten transitions studied. The analytic procedure used was to equate the reduced photon energy $(h\nu)/a$ to the reduced energy difference for the levels in question as expressed by the polynomial expansions given in Appendix A. A quadratic equation in x was thereby obtained and solved numerically. Five values of x were thus obtained for the three $\Delta M_J=\pm 1$ and two $\Delta M_J=\pm 2$ transitions. These calculated values of x were then converted to equivalent proton resonance frequencies. Since the position of the proton probe was different from the position of the paramagnetic sample, the calculated proton resonance frequencies could not agree with the measured frequencies and, in fact, the calculated frequencies were higher by approximately 0.5 G, which is the expected field gradient for the physical configuration in question. It was therefore more meaningful to compare the difference between two calculated proton resonance frequencies and the corresponding measured frequencies and so this was done. The average difference for two runs corresponding to 20 resonance determinations was 550 cps for an average proton resonance frequency of approximately 21×10^6 cps. Taking an estimate of the random error as one half of the average difference, because of the subtraction of frequencies in the analysis, gave an agreement within approximately 13 parts per million. This result is within the expected uncertainty arising from field jitter and uncertainty in specifying the proton resonance at the midpoint of the proton modulation cycle. The conclusion reached, is therefore, that within the precision of this experiment the resonances are correctly interpreted as arising from single- and two-quantum transitions within the hyperfine multiplet calculations presented in Sec. IIA.

B. Power Dependence of Two-Quantum Transitions

Using the results of the variation-of-constants calculation of the first- and second-order probability amplitudes for the $\Delta M_J=\pm 1$ and $\Delta M_J=\pm 2$ transitions, respectively, the expected ratio of intensity of the two-quantum transition to the single-quantum transition

with no saturation is

$$\left|\frac{a_{\frac{1}{2}}^{(2)}}{a_{\frac{1}{2}}^{(1)}}\right|^2=\frac{1}{\hbar^2}\frac{|\langle\frac{1}{2}|\mathcal{H}'(0)|-\frac{1}{2}\rangle|^2}{(\frac{1}{2}\omega_{\frac{1}{2}-\frac{3}{2}}-\omega_{-\frac{1}{2}-\frac{3}{2}})^2} \tag{7}$$

for a particular pair of transitions. For the resonances discussed here the frequency difference in the denominator expressed as a difference in magnetic resonance fields is approximately 5.6 G. For low microwave power this intensity ratio will be very small and the two-quantum transition will be unobservably small compared with the single-quantum transition. The intensity ratio should rise linearly with the microwave power until saturation conditions are reached. The two-quantum transitions will saturate more rapidly, since their linewidth is half that of the single quantum transition. Figure 4 is a plot of the average intensity ratio of two-quantum to single-quantum transitions as a function of microwave power. The average ratio is taken to be the sum of the peak-to-peak amplitudes of both two-quantum transitions divided by the sum of the central and one adjoining single-quantum transition. The data plotted are taken from the runs shown in Fig. 2. As expected, the curve shows essentially a linear power dependence of the intensity ratio above a threshold power level established by system sensitivity. With high power, saturation becomes important.

C. Intensities of the $\Delta M_J=\pm1$ Transitions

The peak-to-peak amplitude of the center line of each $\Delta M_J=\pm1$ triplet is greater than the amplitude of the outer lines of each triplet, which are equal. The experimental values for the ratio of center-line amplitude to outer-line amplitude decrease from 1.4 at very low power to 1.04 at the highest power used, decreasing in a continuous manner with increasing power. This behavior can be understood by considering the Schwinger-Karplus[10] expression for the line shape of a microwave transition of the type considered here. Their expression for the line shape is

$$f(\omega,\omega_{mn})=\frac{\tau^{-1}|\mathfrak{y}\cdot\mathbf{H}_{rf}|_{mn}^2}{(\omega-\omega_{mn})^2+\tau^{-2}+\hbar^{-2}|\mathfrak{y}\cdot\mathbf{H}_{rf}|_{mn}^2}.$$

In the absence of saturation, any variation in intensity between the resonances discussed here will arise from the dipole-moment matrix element in the numerator, $|\langle jm|J_+|jm-1\rangle|^2=(j-m+1)(j+m)$. The ratio of this term for the center and outer lines of the $\Delta M_J=\pm1$ triplet is $\frac{4}{3}=1.33$; this agrees with the low-power experimental value of 1.4. With higher power, the saturation term in the denominator, $|\mathfrak{y}\cdot\mathbf{H}_{rf}|_{mn}^2$ decreases the amplitude of $f(\omega_i\omega_{mn})$. This decrease will be greater for the central line of the triplet, since, as we have shown, the square of the dipole-moment matrix element is larger by a factor of $\frac{4}{3}$. Consequently, it is expected that the amplitude difference between central and outer lines of the $\Delta M_J=\pm1$ triplet will decrease with increasing microwave power, as has been observed.

[10] R. Karplus and J. Schwinger, Phys. Rev. **73**, 1020 (1948).

D. Relative Intensities of $\Delta M_J=\pm2$ Resonances

Experimentally, we found that the two-quantum transition occurring at higher magnetic field

$$(M_J=-\tfrac{3}{2}\leftrightarrow M_J=+\tfrac{1}{2})$$

has greater intensity than the transition occurring at lower magnetic field

$$(M_J=-\tfrac{1}{2}\leftrightarrow M_J=+\tfrac{3}{2}).$$

The observed ratio of intensity of high-field to low-field two-quantum transition is 1.34 for Cl^{35} and 1.27 for Cl^{37}. As discussed in Sec. IIB, the intensities should vary as $|a_{\frac{1}{2}}^{(2)}(t)|^2$ and $|a_{\frac{3}{2}}^{(2)}(t)|^2$, the expressions for these quantities being given in Eqs. (5) and (6). The numerators of these expressions contain the matrix element

$$\langle\tfrac{1}{2}|J_+|-\tfrac{1}{2}\rangle\langle-\tfrac{1}{2}|J_+|-\tfrac{3}{2}\rangle \text{ and } \langle\tfrac{3}{2}|J_+|\tfrac{1}{2}\rangle\langle\tfrac{1}{2}|J_+|-\tfrac{1}{2}\rangle,$$

which are equal. No intensity difference can arise, therefore, from the transition matrix element. The other relevant factor in the a's is the frequency difference in the denominator. This factor is the difference between the photon frequency and the frequency of the "first step" in the two-quantum absorption. We look, therefore, for an intensity variation from the factor

$$\left|\frac{a_{\frac{1}{2}}^{(2)}}{a_{\frac{3}{2}}^{(2)}}\right|^2=\left|\frac{(\omega-\omega_{\frac{1}{2}-\frac{1}{2}})}{(\omega-\omega_{-\frac{1}{2}-\frac{3}{2}})}\right|^2. \tag{8}$$

This ratio was evaluated from the known photon frequency and the calculated frequency of the "first step" transition by using the eigenvalue series expansions and the known values of x at resonance. The calculated intensity ratios are 1.39 for Cl^{35}, and 1.31 for Cl^{37}, which gives good agreement with experiment.

E. Linewidths of $\Delta M_J=\pm2$ Transitions

As discussed by Hughes and Geiger,[7] the expressions for the probability amplitudes $a_{M_J}^{(2)}(t)$, Eqs. (5), (6) predict a linewidth for the $\Delta M_J=\pm2$ transitions of half of that of the $\Delta M_J=\pm1$ transitions. As can be seen from Fig. 2, this was observed experimentally.

ACKNOWLEDGMENTS

The author would like to gratefully acknowledge the support provided by the resources and facilities of the Microwave Spectroscopy Laboratory of the Research Laboratory of Electronics. The X-band spectrometer used in this experiment was the standard spectrometer of this laboratory. John D. Kierstead and Sayfollah B. Afshartous are to be thanked for their assistance with the experiments and with taking data. Professor David R. Whitehouse loaned us the Hewlett-Packard Transfer Oscillator and the Hewlett-Packard Frequency Converter both of which were very much appreciated. Miss Mida N. Karakashian and Miss Elizabeth J. Cambell of the Joint Computing Group, MIT, are to be thanked for programing the eigenvalue problem and seeing it through. Finally, the Computation Center, MIT, is to be thanked for providing time on the computer for the eigenvalue program.

APPENDIX A

As explained in the text, Sec. II, the eigenvalue problem of the reduced Hamiltonian was programed and solved on the MIT IBM 709 Computer. The eigenvalues are obtained as power series expansions in $x=g_J\mu_0 H_z/ha$. The numerical values for the parameters c and α that were defined in Sec. II are given here for each of the two isotopes. The range in x for which the polynomials represent a least-squares fit to $1:10^6$ is indicated for each isotope also.

Cl^{35} $\quad \alpha=0.223685\times10^{-3}$; $\quad c=0.267612$

M_J	M_I	Polynomial eigenvalue $(40\leq x\leq 46)$
$\frac{3}{2}$	$\frac{3}{2}$	$2.316903 + 1.50033553x$
$\frac{3}{2}$	$\frac{1}{2}$	$0.86901164+1.4957920x+0.33443613\times10^{-4}x^2$
$\frac{3}{2}$	$-\frac{1}{2}$	$-0.59367231+1.4945862x+0.41532171\times10^{-4}x^2$
$\frac{3}{2}$	$-\frac{3}{2}$	$-2.0373559 +1.4961546x+0.27660517\times10^{-4}x^2$
$\frac{1}{2}$	$\frac{3}{2}$	$0.49712389 +0.50465860x-0.33488876\times10^{-4}x^2$
$\frac{1}{2}$	$\frac{1}{2}$	$0.29224395 +0.50087606x-0.66565343\times10^{-5}x^2$
$\frac{1}{2}$	$-\frac{1}{2}$	$-0.049036121+0.49689940x+0.22625953\times10^{-4}x^2$
$\frac{1}{2}$	$-\frac{3}{2}$	$-0.59396607 +0.49437571x+0.41384716\times10^{-4}x^2$
$-\frac{1}{2}$	$-\frac{3}{2}$	$0.86907202-0.50465872x+0.33490513\times10^{-4}x^2$
$-\frac{1}{2}$	$-\frac{1}{2}$	$0.29219691-0.49934555x-0.66783485\times10^{-5}x^2$
$-\frac{1}{2}$	$\frac{1}{2}$	$-0.34427185-0.49605450x-0.30019072\times10^{-4}x^2$
$-\frac{1}{2}$	$\frac{3}{2}$	$-1.0151464 -0.49514143x-0.34712166\times10^{-4}x^2$
$-\frac{3}{2}$	$-\frac{3}{2}$	$2.316903 -1.50033553x$
$-\frac{3}{2}$	$-\frac{1}{2}$	$0.49722175-1.4957938x-0.33424295\times10^{-4}x^2$
$-\frac{3}{2}$	$\frac{1}{2}$	$-1.0153650 -1.4953551x-0.34823223\times10^{-4}x^2$
$-\frac{3}{2}$	$\frac{3}{2}$	$-2.3021966 -1.4969776x-0.20519864\times10^{-4}x^2$

Cl^{37} $\quad \alpha=0.186204\times10^{-3}$; $\quad c=0.253361$

M_J	M_I	Polynomial eigenvalue $(49\leq x\leq 55)$
$\frac{3}{2}$	$\frac{3}{2}$	$2.31334025+1.5002793x$
$\frac{3}{2}$	$\frac{1}{2}$	$0.83834989+1.4971928x+0.18479538\times10^{-4}x^2$
$\frac{3}{2}$	$-\frac{1}{2}$	$-0.63047548+1.4963201x+0.23256223\times10^{-4}x^2$
$\frac{3}{2}$	$-\frac{3}{2}$	$-2.0673948 +1.4973609x+0.15334545\times10^{-4}x^2$
$\frac{1}{2}$	$\frac{3}{2}$	$0.53394851 +0.50321876x-0.18855929\times10^{-4}x^2$
$\frac{1}{2}$	$\frac{1}{2}$	$0.29675613 +0.50051653x-0.30373363\times10^{-5}x^2$
$\frac{1}{2}$	$-\frac{1}{2}$	$-0.074441892+0.49781736x+0.13163987\times10^{-4}x^2$
$\frac{1}{2}$	$-\frac{3}{2}$	$-0.63109763 +0.49615882x+0.23009683\times10^{-4}x^2$
$-\frac{1}{2}$	$-\frac{3}{2}$	$0.8392752 -0.50321445x+0.18815248\times10^{-4}x^2$
$-\frac{1}{2}$	$-\frac{1}{2}$	$0.29665412-0.49966521x-0.30845920\times10^{-5}x^2$
$-\frac{1}{2}$	$\frac{1}{2}$	$-0.31744481-0.49733898x-0.16627929\times10^{-4}x^2$
$-\frac{1}{2}$	$\frac{3}{2}$	$-0.97912344-0.49657774x-0.20013306\times10^{-4}x^2$
$-\frac{3}{2}$	$-\frac{3}{2}$	$2.31334025-1.5002793x$
$-\frac{3}{2}$	$-\frac{1}{2}$	$0.53464419-1.4971804x-0.18597662\times10^{-4}x^2$
$-\frac{3}{2}$	$\frac{1}{2}$	$-0.97958915-1.4967460x-0.20185368\times10^{-4}x^2$
$-\frac{3}{2}$	$\frac{3}{2}$	$-2.2881504 -1.4978089x-0.12160268\times10^{-4}x^2$

PHYSICAL REVIEW VOLUME 127, NUMBER 3 AUGUST 1, 1962

Second-Order Quadrupole Effect for the Nuclear Hexadecapole Coupling in Ions*

R. M. STERNHEIMER
Brookhaven National Laboratory, Upton, New York
(Received March 21, 1962)

In connection with the possible existence of a nuclear electric hexadecapole moment, and the resulting large induced hexadecapole moment for medium and heavy ions due to antishielding effects, expressions have been obtained for the additional induced hexadecapole moment, $H_{\text{ind}}{}^Q$, due to the perturbation of the ion by the field of the nuclear quadrupole moment Q taken in second order. $H_{\text{ind}}{}^Q$ is proportional to Q^2. Numerical results for some of the terms of $H_{\text{ind}}{}^Q$ are presented for the Cu^+, Ag^+, and Hg^{++} ions.

I. INTRODUCTION

THE antishielding of ions for a possible nuclear electric hexadecapole moment H has been discussed in two previous papers.[1,2] It has been shown that the relevant antishielding factor η_∞, which gives the HDM (hexadecapole moment) induced in the ion core $H_{\text{ind}}=-\eta_\infty H$, will be very large for medium and heavy ions. Thus, it was found that for Cu^+, Ag^+, and Hg^{++}, η_∞ has the values $\eta_\infty(Cu^+)=-1200$, $\eta_\infty(Ag^+)=-8050$, and $\eta_\infty(Hg^{++})=-63\,000$.

It has been recently pointed out by Foley[3] that the interaction of the nuclear quadrupole moment Q taken in second order will also contribute to hexadecapole effects. For the present case of ions, we are interested

* Work performed under the auspices of the U. S. Atomic Energy Commission.
[1] R. M. Sternheimer, Phys. Rev. Letters **6**, 190 (1961).
[2] R. M. Sternheimer, Phys. Rev. **123**, 870 (1961).
[3] H. M. Foley (private communication).

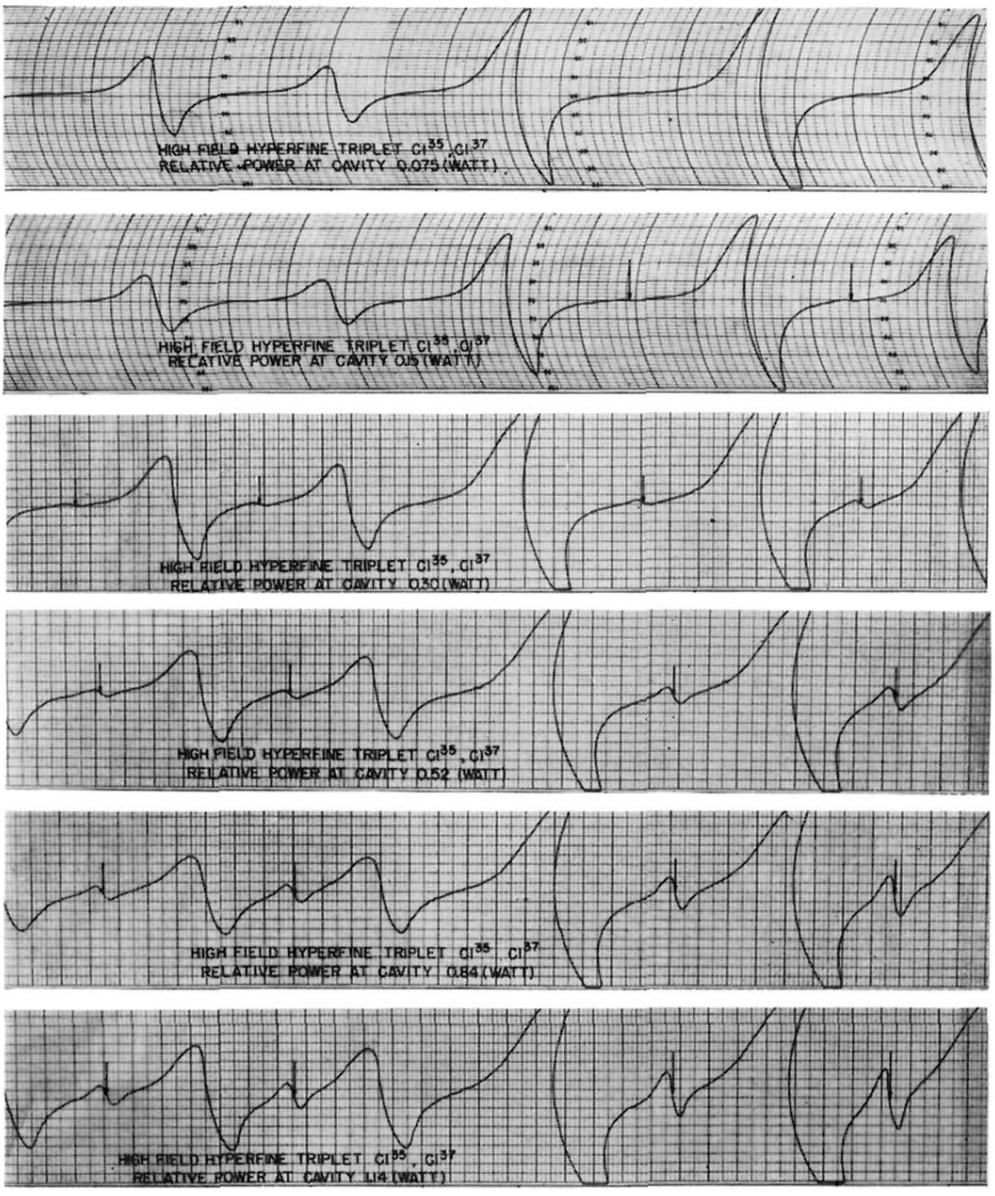

FIG. 2. Microwave transitions for $M_I = -\frac{3}{2}$ and $\Delta M_J = \pm 1$ in atomic chlorine. Resonances for both isotopes are shown; the more intense triplet corresponds to Cl^{35} which is 75% abundant. This figure shows the onset of the two-quantum transitions with increasing microwave power.